

4 Interferometers

We have looked at the details of interference patterns in the previous section, but in these cases the patterns produced have been fixed, so they can be explained, but there is not much scope for actually using them. An interferometer is a device which produces a variable interference pattern which can be controlled by varying the optical path length between the interfering beams in some manner.

The two examples in this section both use amplitude division of a common light source and the resulting fringe patterns can be used to investigate a variety of topics. For example they can be used to measure the refractive index n of materials, or the thickness of materials if very thin. It is also the case that many spectral lines from light emitted by atoms are in fact a series of very closely separated lines, and interferometers can be used to find and measure these small separations.

4.1 The Michelson Interferometer

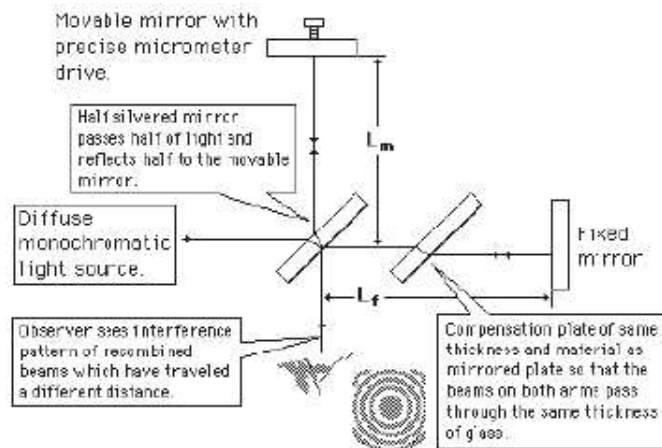


Figure 28: The experimental set-up for the Michelson interferometer.

This is an apparatus which splits a single beam into two equal amplitude parts, which travel down two arms of the interferometer at right angles to each other. One of the beams hits a fixed mirror and is reflected and one a movable mirror. By altering the position of the movable mirror one controls the path difference. The apparatus is shown in detail in figure 28. The amplitude division is made by the beam splitter. One slight complication is that one beam travels through the splitter three times and the other only once. In order to make the path of each beam through glass the same a compensator plate of the same thickness as the beam splitter is added to the second path. This is mainly important if we use light of different wavelengths where n_{glass} may be slightly wavelength dependent, and add a λ -dependent phase difference if the path difference in glass is not the same for each beam.

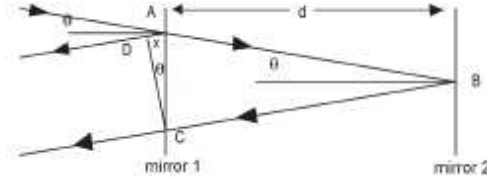


Figure 29: The details of the path difference between the two beams for the Michelson interferometer.

The path difference between the two beams is illustrated in figure 29. It is exactly the same situation as for reflection from two successive boundaries in the previous section, except that it has been achieved without the need for two materials of different refractive index and with a path difference which is variable. As can be seen from the figure, and using exactly the same argument as in eqs. (57-60) in Section 3.2, if the distance between the length of the two arms of the interferometer is $L_f - L_m = d$, then the path difference introduced for light which strikes the mirrors at angle θ to the normal is

$$\Delta = 2dn \cos \theta, \quad (82)$$

where the arms of the interferometer are usually filled with air, so we assume $n = 1$ to a good approximation. There is also one extra phase shift of π in the beam which strikes the fixed mirror, coming from the reflection off the back of the beam splitter. This means that there is constructive interference and bright fringes when

$$2d \cos \theta = (m + \frac{1}{2})\lambda \quad \rightarrow \quad \cos \theta = \frac{(m + \frac{1}{2})\lambda}{2d}, \quad (83)$$

where m is an integer. There is destructive interference, i.e. dark fringes, when

$$2d \cos \theta = m\lambda \quad \rightarrow \quad \cos \theta = \frac{m\lambda}{2d}. \quad (84)$$

As with Young's double slits we can be more quantitative. Assuming that the beam is indeed split exactly into two equal amplitude parts then the total amplitude detected is

$$\begin{aligned} A &= E \exp(i2kL_m) + E \exp(i2kL_m + ik\Delta + i\pi) \\ &= E \exp(i2kL_m) - E \exp(i2kL_m + ik\Delta) \\ &= e^{(i2kL_m + ik\Delta/2)} (E \exp(ik\Delta/2) - E \exp(-ik\Delta/2)) \\ &= -2iE e^{(i2kL_m + ik\Delta/2)} \sin(k\Delta/2), \end{aligned} \quad (85)$$

where we have used $\exp(i\pi) = -1$. The intensity is proportional to the amplitude squared so

$$I(\theta) \propto 4|E|^2 \sin^2(k\Delta/2)$$

$$\rightarrow I(\theta) = 4I_0 \sin^2((2\pi/\lambda)d \cos \theta), \quad (86)$$

where I_0 is the intensity from one wave, $I_0 \propto |E|^2$. The pattern is hence of the same form as for Young's slits, with the intensity falling to exactly half when halfway between the brightest and darkest part of the pattern. As d increases the value of θ for a given fringe increases so they expand outwards and new fringes appear at the centre. Hence, rings appear from the centre and expand, a new one appearing every time $(2\pi/\lambda)d \cos \theta$ increases by π , i.e. a new one appears at the centre ($\cos \theta = 1$) for each increase in d of $\lambda/2$. A slightly idealised version of this is shown in figure 30. In practice a less than perfect interferometer will result in less clear fringes.

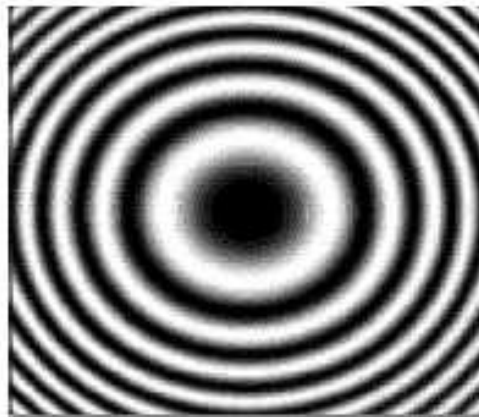


Figure 30: The (slightly idealised) pattern of fringes from a Michelson interferometer using monochromatic light.

4.1.1 Measurement of Refractive Index

If we have air in the arms of the interferometer, and then we introduce an object of refractive index n and thickness t , the optical path of that arm will increase by an amount $(n - n_{\text{air}})t$. The light goes through the object twice, so the optical path difference between the two arms changes by $2(n - n_{\text{air}})t$. Therefore the pattern changes by

$$\frac{2(n - n_{\text{air}})t}{\lambda} \quad (87)$$

fringes. Hence, we can use this result to measure the refractive index of the object, or if this is known to high accuracy already, measure the thickness of objects accurate to less than the wavelength of light.

4.1.2 Resolution of Spectral Lines

Many well-known spectral lines arising from atomic transitions are in fact a series of very closely separated lines. If a source has two lines λ_1 and λ_2 where $\Delta\lambda = \lambda_2 - \lambda_1 \ll \lambda_1$ then we obtain a very slightly different diffraction pattern

for the two lines. We can choose $2d \cos \theta$ so that it gives a bright fringe for each, e.g. if this is at the centre ($\theta = 0$)

$$2d = (p_1 + \frac{1}{2})\lambda_1 = (p_2 + \frac{1}{2})\lambda_2, \quad (88)$$

for two different integers p_1 and p_2 . Consequently, p_1, p_2 satisfy

$$p_1 - p_2 = 2d \left(\frac{1}{\lambda_1} - \frac{1}{\lambda_2} \right). \quad (89)$$

As d varies the patterns diverge, but we will next get coincident bright fringes at the centre when the difference between the integers increases by exactly one unit. When this happens

$$p_1 - p_2 + 1 = 2(d + \Delta d) \left(\frac{1}{\lambda_1} - \frac{1}{\lambda_2} \right) = 2(d + \Delta d) \frac{\Delta \lambda}{\lambda_1 \lambda_2}. \quad (90)$$

Therefore, this happens if

$$1 = \frac{2\Delta \lambda \Delta d}{\lambda_1 \lambda_2}, \quad (91)$$

which leads to

$$\Delta \lambda = \frac{\lambda_1 \lambda_2}{2\Delta d} \approx \frac{\lambda_1^2}{2\Delta d}. \quad (92)$$

So in principle we are able to resolve any two wavelengths if we vary the separation between the two mirrors sufficiently to return to the original comparison between patterns. In fact we wish to do this over a distance such that the pattern repeats a number of times and then to divide the total Δd by the number of pattern repeats for maximum accuracy. However, in practice this is limited by $\Delta \lambda$. If this is sufficiently small one pattern repeat may not be possible due to finite coherence of the light source.

4.2 Fabry-Perot Interferometer (Etalon)

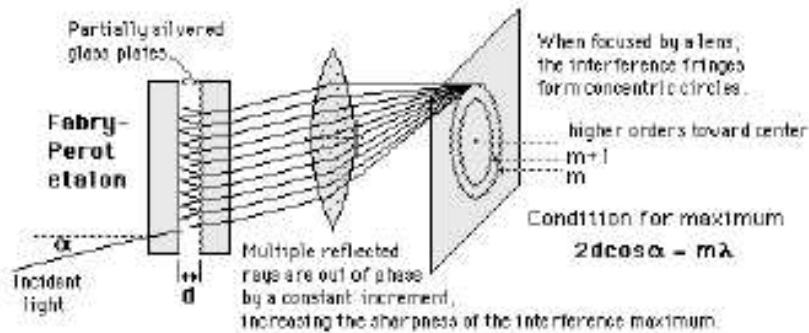


Figure 31: The experimental set up for the Fabry-Perot etalon.

The Fabry-Perot interferometer, or etalon, makes use of multiple reflections between two closely separated mirrored surfaces, as shown in figure 31. At each

stage part of the light is transmitted but the majority is reflected back into the etalon. This leads to a larger number of interfering waves than the two we have considered in each of our previous examples. In principle it can be an infinite number, but the amplitude of each successive wave falls, so at some point the amplitude will become negligible. This depends on the size of the reflection coefficients r for the amplitude of the light reflected.

The general condition for bright fringes is as before that there is a constant path difference between successive beams, i.e. if the light enters at angle θ to the normal to the etalon plates, separated by a distance t , then we require $2t \cos \theta = m\lambda$, where m is an integer (this time there is a phase change of π from both reflections, so overall each beam has a change of 2π , which is the same as no phase change). Each successive transmitted beam has amplitude $|r|^2 \exp(i2kt \cos \theta) \equiv R \exp(i2\gamma)$, compared to the previous one, where $\gamma = kt \cos \theta \equiv (2\pi/\lambda)t \cos \theta$, and R is the reflectance. One can show that this results in an transmitted intensity of the form

$$I = I_{\max} \times \frac{1}{1 + F \sin^2 \gamma}, \quad (93)$$

where $F = 4R/(1 - R)^2$ is defined to be the finesse of the etalon. It is a large number, e.g. for $R = 0.9$ we obtain $F = 360$.

The maximum transmitted amplitude $I = I_{\max}$ when $\sin \gamma = 0$, i.e. when

$$\gamma = \frac{2\pi}{\lambda} t \cos \theta = m\pi \quad \rightarrow \quad 2t \cos \theta = m\lambda. \quad (94)$$

Small values of m means small $\cos \theta$, i.e. wide angles. In fact there is formally a fringe at $m = 0$ but this will never be seen in practice since it is at right angles to the etalon where no light is transmitted. The lowest order fringe is for $m = 1$. As t increases we can obtain more fringes.

The fringes produced by the Fabry-Perot interferometer are far sharper than the Michelson interferometer or in Young's double slits. The intensity never becomes zero, the minimum relative value being $1/(1 + F)$, but this is very small for large F . However, the intensity falls to half its maximum when

$$\frac{1}{1 + F \sin^2 \gamma} = \frac{1}{2} \quad \rightarrow \quad \sin \gamma = \pm 1/\sqrt{F}, \quad (95)$$

where $1/\sqrt{F} \ll 1$. Let us say this happens at $\gamma = \gamma_{\max} + \Delta\gamma$, where $\gamma_{\max} = m\pi$. This results in

$$\sin(\gamma_{\max} + \Delta\gamma) = \sin \gamma_{\max} \cos \Delta\gamma + \sin \gamma_{\max} \cos \Delta\gamma = \pm 1/\sqrt{F}. \quad (96)$$

But $\sin \gamma_{\max} = 0$ and $\cos \gamma_{\max} = \pm 1$ and so

$$\sin \Delta\gamma \approx \Delta\gamma = \pm 1/\sqrt{F}. \quad (97)$$

This results in very narrow bands if F is large and is illustrated in figure 32.

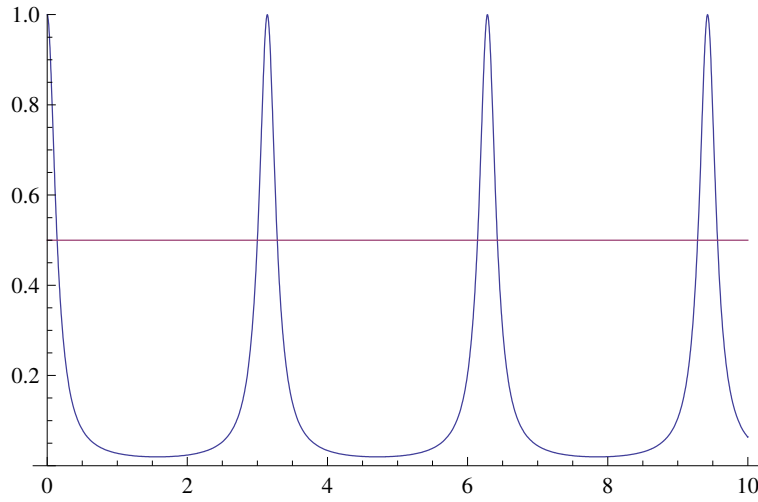


Figure 32: The pattern of intensity from the Fabry-Perot etalon. The x -axis is in units of $\gamma = (\pi/\lambda)2t \cos \theta$. The line showing half-maximum intensity is included.

4.2.1 Chromatic Resolution of a Fabry-Perot Interferometer

If we have two lines of similar wavelength, i.e. λ_1 and λ_2 with $\lambda_2 - \lambda_1 = \Delta\lambda$, the interferometer is deemed to be just able to resolve the fringes at a given order m if the maximum of one falls at the same place as the half-maximum of the other. If we consider the distance from maximum to half-maximum for one wavelength λ_1 then we saw in the previous section that this is given by $\Delta\gamma = \pm 1/\sqrt{F}$, where $\gamma = (2\pi/\lambda_1)t \cos \theta$. For fixed λ_1 and t this means

$$\Delta(\cos \theta) = \pm \frac{\lambda_1}{\sqrt{F}2\pi t}. \quad (98)$$

But maxima are defined to be at $2t \cos \theta = m\lambda$, so the change in the angle at which a maximum is seen as a function of wavelength is

$$2t\Delta(\cos \theta) = m\Delta\lambda \quad \rightarrow \quad \Delta \cos \theta = \frac{m\Delta\lambda}{2t}. \quad (99)$$

Equating the two expressions for $\Delta \cos \theta$ we obtain

$$|\lambda_1/\Delta\lambda| = m\pi\sqrt{F}, \quad (100)$$

which defines the chromatic resolving power of the interferometer. It improves with increasing order of the fringe and increasing reflectance. The former can be increased by making t larger, so allowing fringes of higher order.